

Negative phase advance in polarization independent, multi-layer negative-index metamaterials

Koray Aydin, Zhaofeng Li, Levent Sahin, and Ekmel Ozbay

Nanotechnology Research Center, Department of Physics and Department of Electrical and Electronics Engineering,
Bilkent University, Bilkent, 06800, Ankara, Turkey
aydin@fen.bilkent.edu.tr

Abstract: We demonstrate a polarization independent negative-index metamaterial (NIM) at microwave frequencies. Transmission measurements and simulations predict a left-handed transmission band with negative permittivity and negative permeability. A negative-index is verified by using the retrieval procedure. Effective parameters of single-layer and two-layer NIMs are shown to be different. Negative phase advance is verified within the negative-index regime by measuring the phase shift between different sized negative-index metamaterials. Backward wave propagation is observed in the numerical simulations at frequencies where the phase advance is negative.

©2008 Optical Society of America

OCIS codes: (160.3918) Materials : Metamaterials; (260.2065) Physical optics : Effective medium theory

References and links

1. E. Ozbay, K. Aydin, and K. Guven, "Metamaterials with negative permeability and negative refractive index: experiments and simulations," *J. Opt. A: Pure and Appl. Opt.* **9**, S301-S307 (2007).
2. C. M. Soukoulis, M. Kafesaki, and E. N. Economou, "Negative index materials: New frontiers in optics," *Adv. Mater.* **18**, 1941-1952 (2006).
3. V. M. Shalaev, "Optical negative-index metamaterials," *Nature Photonics* **1**, 41-48 (2007).
4. D. R. Smith, J. B. Pendry, and M. C. K. Wiltshire, "Metamaterials and negative refractive index," *Science* **305**, 788-792 (2004).
5. J. B. Pendry, A. J. Holden, D. J. Robbins, and W. J. Stewart, "Magnetism from conductors and enhanced nonlinear phenomena," *IEEE Trans. Microwave Theory Tech.* **47**, 2075-2084 (1999).
6. K. Aydin, K. Guven, C. M. Soukoulis, and E. Ozbay, "Observation of negative refraction and negative phase advance in left-handed metamaterials," *Appl. Phys. Lett.* **86**, 124102 (2005).
7. K. Aydin, K. Guven, M. Kafesaki, L. Zhang, C. M. Soukoulis, and E. Ozbay, "Experimental observation of true left-handed transmission peak in metamaterials," *Opt. Lett.* **29**, 2623-2625 (2004).
8. K. Aydin, I. Bulu and E. Ozbay, "Subwavelength resolution with a negative-index metamaterial superlens," *Appl. Phys. Lett.* **90**, 254102 (2007).
9. M. Gokkavas, K. Guven, I. Bulu, K. Aydin, M. Kafesaki, R. Penciu, C. M. Soukoulis, and E. Ozbay, "Experimental demonstration of a left-handed metamaterial operating at 100 GHz," *Phys. Rev. B* **73**, 193103 (2006).
10. T. J. Yen, W. J. Padilla, N. Fang, D. C. Vier, D. R. Smith, J. B. Pendry, D. N. Basov, and X. Zhang, "Terahertz magnetic response from artificial materials," *Science* **303**, 1494-1496 (2004).
11. S. Linden, C. Enkrich, M. Wegener, J. Zhou, T. Koschny, and C. M. Soukoulis, "Magnetic response of metamaterials at 100 THz," *Science* **306**, 1351-1353 (2004).
12. J. Zhou, T. Koschny, M. Kafesaki, E. N. Economou, J. B. Pendry, and C. M. Soukoulis, "Saturation of magnetic response of split-ring resonators at optical frequencies," *Phys. Rev. Lett.* **95**, 223902 (2005).
13. V. M. Shalaev, W. Cai, U. K. Chettiar, Hsiao-Kuan Yuan, A. K. Sarychev, V. P. Drachev, and A. V. Kildishev, "Negative index of refraction in optical metamaterials," *Opt. Lett.* **30**, 3356-3358 (2005).
14. G. Dolling, C. Enkrich, M. Wegener, J. F. Zhou, C. M. Soukoulis, and S. Linden, "Cut-wire pairs and plate pairs as magnetic atoms for optical metamaterials," *Opt. Lett.* **30**, 3198-3200 (2005).
15. J. Zhou, L. Zhang, G. Tuttle, T. Koschny, and C. M. Soukoulis, "Negative index materials using simple short wire pairs," *Phys. Rev. B* **73**, 041101 (2006).

16. J. Zhou, E. N. Economou, T. Koschny, and C. M. Soukoulis, "Unifying approach to left-handed material design," *Opt. Lett.* **31**, 3620-3622 (2006).
17. K. Guven, M. D. Caliskan, and E. Ozbay, "Experimental observation of left-handed transmission in a bilayer metamaterial under normal-to-plane propagation," *Opt. Express* **14**, 8685 (2006).
18. S. Zhang, W. Fan, K. J. Malloy, S. R. J. Brueck, N. C. Panoiu, and R. M. Osgood, "Near-infrared double negative metamaterials," *Opt. Express* **13**, 4922 (2005).
19. S. Zhang, W. Fan, N. C. Panoiu, K. J. Malloy, R. M. Osgood, and S. R. J. Brueck, "Experimental demonstration of near-infrared negative-index metamaterials," *Phys. Rev. Lett.* **95**, 137404 (2005).
20. G. Dolling, C. Enkrich, M. Wegener, C. M. Soukoulis, and S. Linden, "Simultaneous negative phase and group advance of light in a metamaterial," *Science* **12**, 892-894 (2006).
21. G. Dolling, M. Wegener, C. M. Soukoulis, and S. Linden, "Negative-index metamaterial at 780 nm wavelength," *Opt. Lett.* **32**, 53-55 (2007).
22. M. Kafesaki, I. Tsiapa, N. Katsarakis, T. Koschny, C. M. Soukoulis, and E. N. Economou, "Left-handed metamaterials: The fishnet structure and its variations," *Phys. Rev. B* **75**, 235114 (2007).
23. V. D. Lam, J. B. Kim, S. J. Lee, and Y. P. Lee, "Left-handed behavior of combined and fishnet structures," *J. Appl. Phys.* **103**, 033107 (2008).
24. J. Zhou, T. Koschny, M. Kafesaki, and C. M. Soukoulis, "Size dependence and convergence of the retrieval parameters of metamaterials," *Photon. Nanostruct: Fundam. Appl.* **6**, 96-101 (2008).
25. G. Dolling, M. Wegener, and S. Linden, "Realization of a three-functional-layer negative-index photonic metamaterial," *Opt. Lett.* **32**, 551-553 (2007).
26. N. Liu, H. Guo, L. Fu, S. Kaiser, H. Schweizer, and H. Giessen, "Three-dimensional photonic metamaterials at optical frequencies," *Nature Materials* **7**, 31 (2008).
27. D. R. Smith, S. Schultz, P. Markos and C. M. Soukoulis, "Determination of effective permittivity and permeability of metamaterials from reflection and transmission coefficients," *Phys. Rev. B.* **65**, 195104 (2002).
28. X. Chen, T. M. Grzegorzczuk, B.-I. Wu, J. Pacheco, Jr., and J. A. Kong, "Robust method to retrieve the constitutive effective parameters of metamaterials," *Phys. Rev. E* **70**, 016608 (2004).
29. T. Koschny, P. Markoš, E. N. Economou, D. R. Smith, D. C. Vier, and C. M. Soukoulis, "Impact of the inherent periodic structure on the effective medium description of left-handed and related metamaterials," *Phys. Rev. B* **71**, 245105 (2005).
30. R. S. Penciu, M. Kafesaki, T. F. Gundogdu, E. N. Economou, and C. M. Soukoulis, "Theoretical study of left-handed behavior of composite metamaterials," *Photon. Nanostruct: Fund. Appl.* **4**, 12-16 (2006).
31. N. Katsarakis, M. Kafesaki, I. Tsiapa, E. N. Economou, and C. M. Soukoulis, "High transmittance left-handed materials involving symmetric split-ring resonators," *Photon. Nanostruct: Fundam. Appl.* **5**, 149-155 (2007).

1. Introduction

The response of a material to an incident electromagnetic wave is determined by the material parameters, dielectric permittivity (ϵ), and magnetic permeability (μ). Although, in ordinary materials both ϵ and μ are positive, it is possible to tailor these electromagnetic parameters in metamaterials, which are artificially engineered composite structures [1-4]. Metamaterials play a key role in accessing the negative and positive values of permittivity and permeability in a controlled manner. In recent years, there has been a growing amount of interest in metamaterials research because metamaterials offer exciting phenomena such as negative refraction, subwavelength imaging, and cloaking. The negative refractive index in metamaterials is a consequence of the effective parameters of permeability and permittivity that are simultaneously negative.

Dielectric permittivity takes the negative values below the plasma frequency. The negative values of permeability are accessible with resonators that strongly respond to the incident magnetic field and cause a resonance in magnetic permeability. Such a magnetic metamaterial, a split ring resonator, was first proposed by Pendry *et al.*[5]. Split ring resonators received a great amount of interest and were widely studied for constructing metamaterials at the microwave [6-8], millimeter wave [9], and terahertz [10,11] frequencies. Split ring resonators are not suitable for the planar configuration of metamaterials, since the incident EM wave has to be parallel to the SRR, provided that the magnetic field is perpendicular to the SRR. The magnetic response of split ring resonators starts to saturate optical frequencies [12], and therefore optical magnetism is not achievable with SRRs. However, it is shown that an alternative structure of metal-dielectric composite provides

magnetic resonance at optical frequencies [13,14]. The structure consists of parallel metal slabs with a dielectric substrate in between, wherein the metal slabs provide the inductance and dielectric spacing that in turn provides the capacitance [13]. Realizations of metamaterials using parallel metal slabs (also known as cut-wire pairs) at microwave frequencies followed soon after [15-17]. Fishnet type metamaterials are also reported to exhibit a negative-index at optical [18-21] and microwave frequencies [22-24]. The advantage of metamaterials with fishnet geometry is that the wires providing for negative permittivity and the slab pairs providing for negative permeability are brought together to produce a combined electromagnetic response.

In the present study, we demonstrate a planar negative-index metamaterial (NIM) that operates independent of the incident polarization due to its symmetric configuration. Single-layer and multi-layer metamaterials are characterized by transmission measurements and simulations. We used a low-loss Teflon substrate and obtained a high transmission from NIM structures with a peak value of -2.4 dB. The retrieved effective parameters are in good agreement with the experimental observations. A negative-index appears at frequencies where both permittivity and permeability are negative. The structure size along the propagation direction is shown to affect the effective parameters. The phase shift from different sizes of the NIM samples are measured, wherein we observe a negative phase shift within the negative-index frequency regime, i.e. phase decreases with the increased NIM size. Phase measurements at the right-handed transmission band show the opposite behavior, in which the phase increases with the increasing number of NIM layers. Finally, we simulated the electric field distribution and studied the wave propagation inside the fishnet metamaterial. Backward wave propagation is verified at the negative-index region.

2. Transmission through a fishnet type metamaterial

The fishnet type metamaterials were previously shown to be possible candidates for planar negative index metamaterials [18-24]. In the present study we employ fishnet geometry to construct a metamaterial operating at microwave frequencies. A schematic of a fishnet unit cell is shown in Fig. 1(a). The highlighted areas are the metallic parts. The metal used to construct the structure is copper with a thickness of 20 μm . The substrate is a Teflon board with a thickness of $t=1$ mm. The unit cell is repeated periodically along the x and y directions with a periodicity of $a_x=a_y=14$ mm.

The structure can be considered as a combination of parallel metal slab pairs with the sizes $w_y \times a_x$, which provide the magnetic resonance and continuous wire pairs with the sizes $w_x \times a_y$ in turn providing the negative permittivity [22]. Here, we chose $w_x = w_y = 7$ mm, and therefore the structure is symmetric in all directions. The structure will then work for TE and TM polarizations, as well as for arbitrary linear polarizations due to the symmetry of the slab and wire pairs. Therefore, the NIM will be functional independent of the incident polarization [22].

The number of layers in a single fishnet metamaterial layer (see the inset of Fig. 2) are $N_x=N_y=10$. We then stacked layers with a periodicity along the z direction, $a_z=2$ mm, which is ten times smaller than the wavelength of operation assuring an effective response along the propagation direction (Fig. 1(b)). Transmission and phase measurements were performed using standard high gain transmitter and receiver horn antennae connected to an Agilent N5230A portable network analyzer, which is capable of measuring S-parameters and phase amplitudes. The wave propagates along the z -direction, with the E -field parallel to the y axis and the H field parallel to the x axis. In these measurements, the distance between the antennae was kept at 35 cm. We first measured the transmission through air, and then used this data as a calibration.

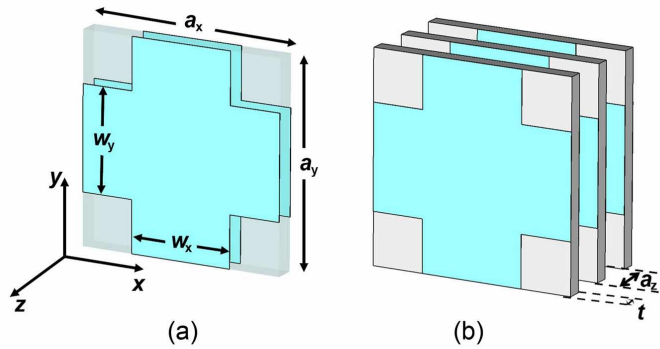


Fig. 1. Schematic drawings of (a) a fishnet unit cell, and (b) a multi-layer fishnet metamaterial structure.

The measured transmission spectrum of a single fishnet metamaterial layer is plotted with a blue line as shown in Fig. 2. We observe a transmission band between 14.2 and 14.8 GHz that is highlighted in Fig. 2. The peak value is -2.4 dB at 14.38 GHz. This band corresponds to a left-handed transmission band, as we will show later on in the following section. We performed numerical simulations in order to check the experimental results. We used the commercially available software, CST Microwave Studio, for the simulations. We simulated the unit cell as shown in Fig. 1(a), with periodic boundary conditions at the x and y axes. Along the propagation direction (z axis), we employed open boundary conditions. Waveguide ports are used to excite and detect electromagnetic waves. The dielectric constant of the Teflon board was taken as $\epsilon=2.16$ with a tangent loss of $\delta=0.005$. The red line in Fig. 2 shows the simulated transmission spectrum of a single layer fishnet structure. The agreement between the theory and experiment is quite good. The transmission peak had a value of -2.9 dB at 14.33 GHz.

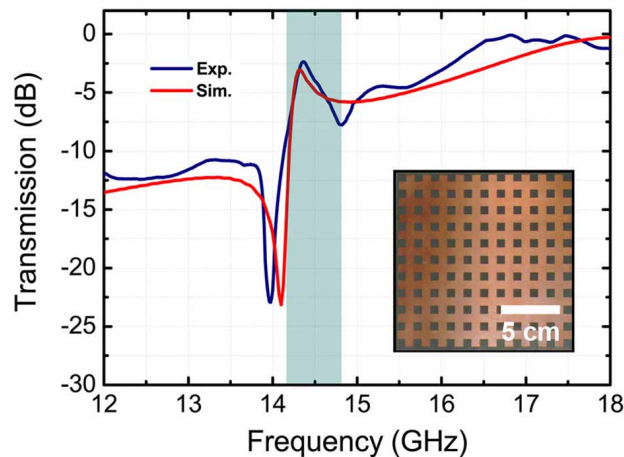


Fig. 2. Measured (blue line) and simulated (red line) transmission spectra of a single layer fishnet metamaterial. The photograph of the real structure is shown in the inset.

Planar metamaterials, where the electromagnetic wave is incident normal to the plane of the metamaterials, were first realized at optical frequencies [18-21]. The characterization of optical negative-index metamaterials were mainly done by using a single layer. It is obvious that the basic properties of metamaterial structures, such as a negative index of refraction, the

negative phase advance cannot be verified by simply using a single layer of the metamaterial. Recently, there have been studies that utilize negative-index metamaterials with more than one layer along the propagation direction [22,25,26]. Here, we report the transmission measurements of a two-layer and five-layer NIM structure. Fig. 3(a) shows the measured (blue line) and simulated (red line) transmission spectra of a two-layer NIM structure. The periodicity along the propagation direction is $a_z = 2$ mm. The transmission band is present with a maximum value of -3.7 dB at 14.38 GHz that is obtained from the measurements. The simulation results predict a similar transmission band where the peak is at 14.33 GHz with a maximum value of -3.0 dB.

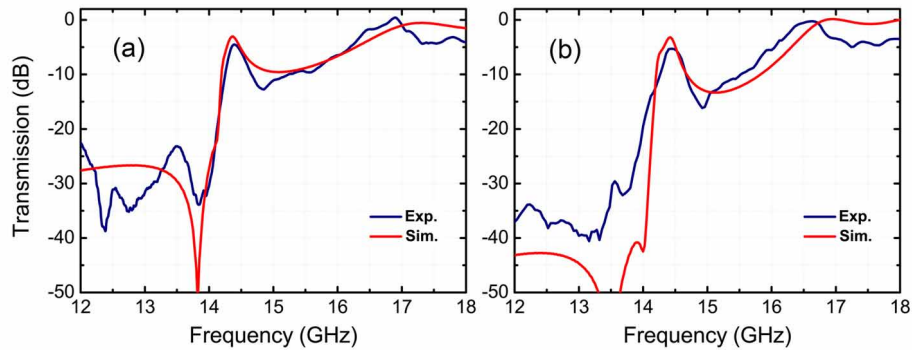


Fig. 3. Measured (blue line) and simulated (red line) transmission spectra of (a) two-layer and (b) five-layer fishnet metamaterial.

Experimental and simulation results of the transmission spectra of five-layer NIM are shown in Fig. 3(b). The transmission peak is at 14.42 GHz, measured as -5.0 dB, and simulated as -3.2 dB. Slight differences between the simulation and experiments can be attributed to the deviation from the ideal material parameters and possible misalignments that may occur during the stacking of the layers. In the simulations, the metamaterial is infinitely periodic along x and y directions, however experimental structure has a finite size which may cause diffraction at the edges. It is noteworthy that increasing the number of layers does not significantly change the transmission value at the left-handed transmission band. This is due to the specific choice of the substrate. The loss mechanism in the fishnet structure is mainly due to the substrate losses. Although the amount of metal is increased by a factor of five, from a one-layer structure to a five-layer structure, the transmission only decreased by -2.6 dB in the measurement. The result is more significant in the simulation results (ideal case) that the transmission peak did not change from a one-layer to a five-layer NIM.

3. Retrieved parameters

One of the most common characterization tools for the metamaterial structures is the retrieval procedure [27-31]. It is widely used to calculate the effective parameters of the metamaterial under investigation. The amplitude and phase of the transmission and reflection are either calculated or measured, in which the real and imaginary parts of the refractive index and wave impedance are then retrieved from the transmission and reflection coefficients. We employed the retrieval procedure to obtain effective permittivity, permeability, and a refractive index. We followed the approach as outlined in Ref. [28]. The advantage of this procedure is that the correct branch of the effective refractive index and effective impedance was selected. The ambiguity in the determination of the correct branch was resolved by using an analytic continuation procedure.

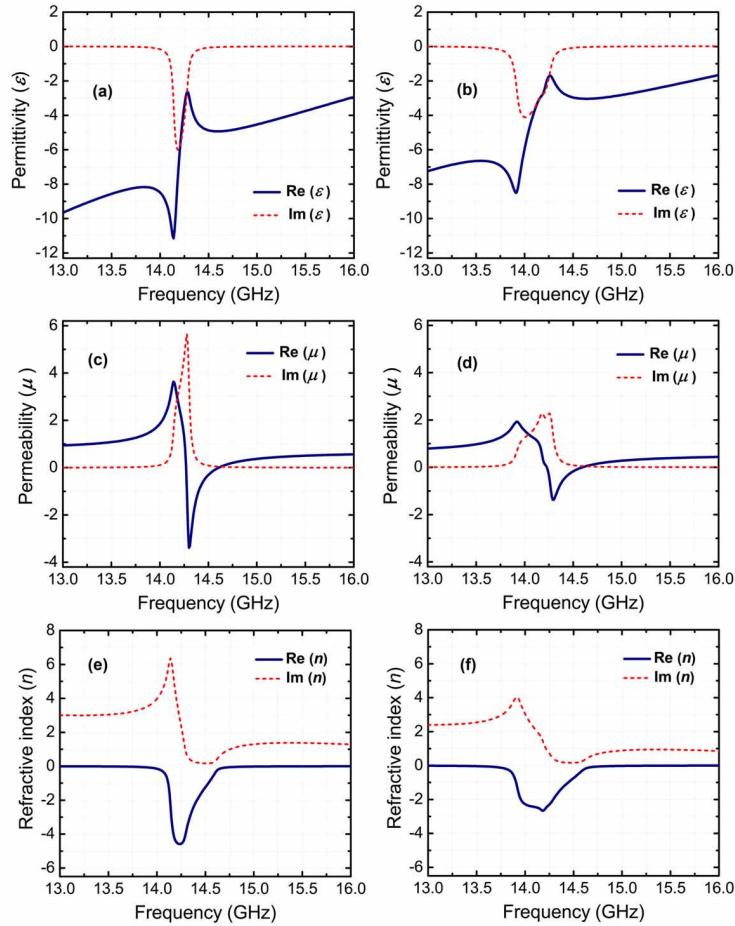


Fig. 4. Retrieved effective parameters of a (left) single-layer and a (right) two-layer fishnet metamaterials. The real (blue line) and imaginary (red dashed line) parts of effective permittivity (top), permeability (middle), and refractive index (bottom) are shown.

In the retrieval procedure, we employed a single layer of NIM along the z axis. Hence, the simulation setup coincides with a slab of NIM that consists of single layer. The effective permittivity and permeability values were then derived from the transmission and reflection coefficients of a single layer of NIM. The real (blue line) and imaginary (red dashed line) parts of the effective permittivity (Fig. 4(a)), permeability (Fig. 4(c)), and index of refraction (Fig. 4(e)) for a single layer of NIM structure was consistent with the simulated and measured transmission spectra. The effective permittivity is negative within the frequency range of interest. The continuous wire arrays that are aligned along the y axis cause plasma oscillations. The plasma frequency of an NIM structure is approx. 16.5 GHz. The resonance in the permittivity at approx. 14.25 GHz is a common characteristic of metamaterials with a negative index. The real part of the magnetic permeability has negative values between 14.23 and 14.65 GHz. The lowest value of μ is -3.38 at 14.3 GHz for a single layer NIM. Since both permeability and permittivity are simultaneously negative, the condition needed in order to have a negative index is satisfied. As seen in Fig. 4(e), the NIM structure possesses negative values of the refractive index within the frequency range 13.95–14.65 GHz.

The retrieval procedure is mainly performed for single unit cells along the propagation direction. However, recent studies have revealed that the geometric size of the structure that

was used to calculate the transmission and reflection coefficients affect the retrieved parameters [24,29]. To check this effect in our fishnet type metamaterial design, we performed further simulations for a two-layer NIM structure. Figures 4(b), 4(d), and 4(f) show the effective permittivity, permeability, and refractive index, respectively. Comparing the results of one-layer and two-layer NIM structure, it is obvious that the real and imaginary parts of ϵ , μ , and n are different. A single layer NIM responds to the incident electromagnetic field stronger than the two-layer structure. We see that the permittivity values were higher for the two-layer NIM structure. The minimum value of permeability for a two-layer NIM was -1.37 at 14.3 GHz. Throughout the frequency range of interest, we found that the absolute values of permittivity and permeability of a one-layer structure is greater than that of a two-layer NIM, i.e. $|\epsilon_{1L}| > |\epsilon_{2L}|$ and $|\mu_{1L}| > |\mu_{2L}|$. Retrieved parameters converge to a value if the metamaterial length employed in the retrieval procedure is equal to the convergence length of the metamaterial [24]. Since two unit cell is below the convergence length of a fishnet metamaterial [24], we found significant difference in the parameters of one and two layer NIM structures. The results reported here are consistent with Zhou *et al.*, in which the authors performed a detailed analysis for the dependence of geometric size and lattice constant on the retrieved parameters of fishnet type metamaterials [24].

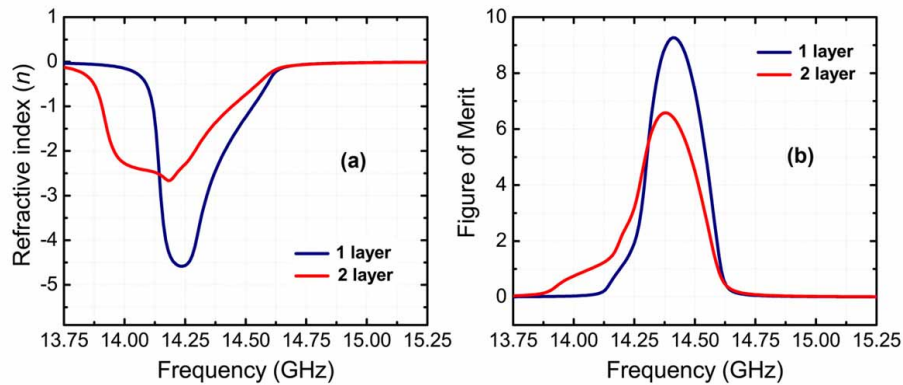


Fig. 5. (a) Real part of retrieved refractive index and (b) figure of merit for a single-layer (blue line) and two-layer metamaterial (red line).

The real parts of the refractive indices of a one and two-layer structure are plotted together in Fig. 5(a). As was expected, the relation between ϵ and μ holds true for the refractive index, since the index depends on ϵ and μ . The minimum values of the refractive index for a one-layer NIM was $n = -4.58$ (at 14.23 GHz) and a two-layer NIM was $n = -2.66$ (at 14.19 GHz). The frequency region between 14.23 and 14.65 GHz was a double negative region, which means that the permeability and permittivity were both negative. We found that the upper edge for the negative index regime was 14.65 GHz for a one and two-layer NIM, where the permeability starts to take on positive values. However, the lower edge is at lower frequencies for a two-layer NIM. Although the refractive index is negative between 13.72 and 14.23 GHz for a two-layer NIM, the permeability is positive within this frequency range. Therefore, the NIM structure behaves like a single negative material [22]. For a one-layer NIM, the single negative frequency region was narrower, in turn appearing between 13.94 and 14.23 GHz.

The figure of merit (FOM) for negative-index metamaterials was defined as a ratio of the absolute value of the real part of an index to the imaginary part of an index, $FOM = |\text{Re}(n)| / \text{Im}(n)$. Figure of merits for one and two-layer NIMs are shown in Fig. 5(b). It is obvious that the figure of merit is larger for a single layer NIM structure. The maximum figure of merit value is 9.26 at 14.41 GHz for a one-layer NIM. For a two-layer structure we found the

highest value of figure of merit to be 6.58 at 14.38 GHz. FOM decreases with the increasing number of layers due to the decrease in the refractive index.

4. Negative phase advance and backward wave propagation

Negative index metamaterials are of special interest for obtaining backward wave propagation, since they inherently have a negative phase advance. A network analyzer is capable of measuring the transmitted phase. We constructed NIM structures with $a_z=2$ mm that have $N_z=2, 3, 4,$ and 5 layers along the propagation direction. The transmitted phase of NIM structures were measured by using the same setup with the transmission measurements. In the measurements, the transmitted phase is calibrated with respect to the phase in free space.

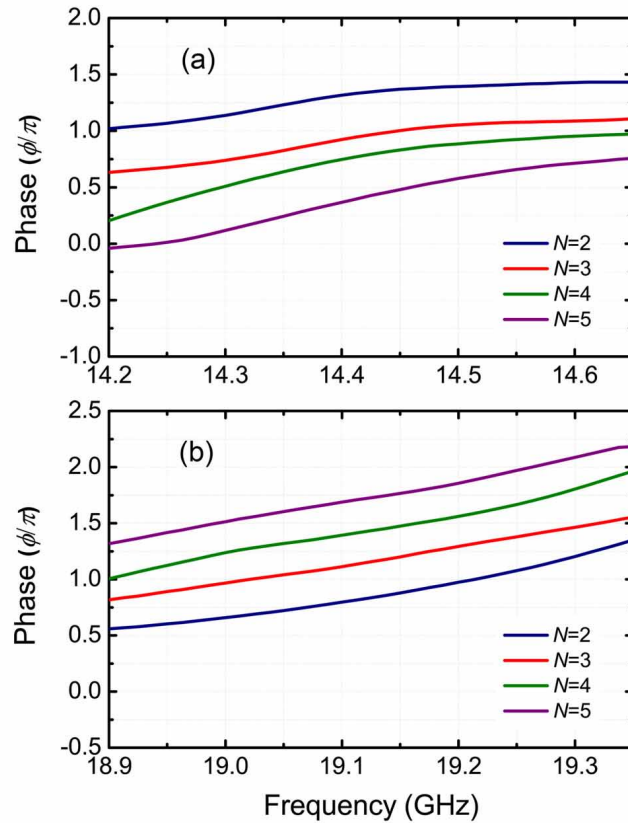


Fig. 6. Transmitted phase of metamaterial structure for two (blue line), three (red line), four (green line), and five (purple line) NIM layers between (a) 14.2 and 14.8 GHz (left-handed transmission regime) and (b) 18.9 and 19.4 GHz (right-handed transmission regime).

Figure 6(a) shows the transmission phase between 14.20 and 14.65 GHz for two (blue line), three (red line), four (green line), and five (purple line) layers of the NIM structure. We plotted the transmitted phase in a narrow band since the transmission below 14.20 GHz and above 14.65 GHz is low and imaginary part of the refractive index is significant (see Fig. 4(f)). The phase decreases between 14.20 and 14.65 GHz with the increasing number of layers along the propagation direction. This is typical behavior for left-handed metamaterials with a negative phase advance [6,17].

We also performed phase measurements at a frequency range where we know that the transmission band has right handed characteristics. The phase spectra for four different NIM structures are shown in Fig. 6(b) at the right-handed transmission region. We observed an increase in the phase with the increasing number of layers along the propagation direction. The negative phase shift for a NIM structure at the negative-index frequency regime means that the phase is directed towards the source. Such behavior is due to the negative phase advance within the interested range of frequencies. These measurements clearly verify the negative phase advance behavior of planar fishnet type multi-layer metamaterials. To our knowledge, this is the first direct observation of negative phase advance for fishnet type NIM structures.

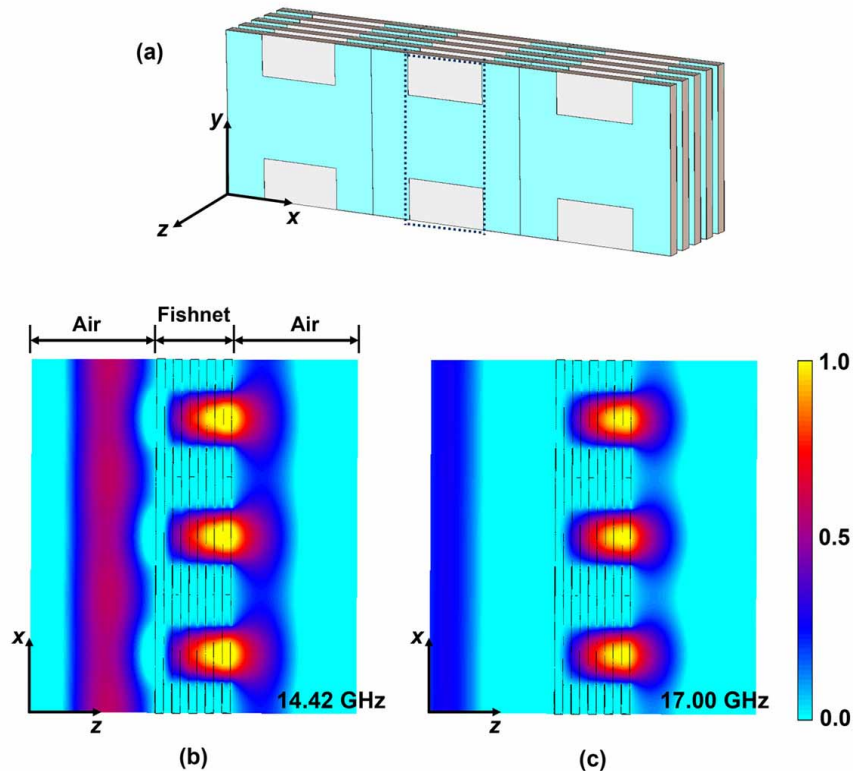


Fig. 7. (a) Schematic drawing of a simulated NIM structure with an alternative unit cell. The structure had three unit cells along x and five unit cells along z axis. (b) Simulated E -field profile at 14.42 GHz where the wave propagates along the $-z$ direction inside the fishnet structure (see video 1) (c) Simulated E -field profile at 17.00 GHz where the wave propagates along the $+z$ direction inside the fishnet structure (see video 2).

Metamaterials with a negative phase advance are also called backward wave materials, since the wave propagation is towards the source inside the metamaterial. We performed numerical simulations using CST Microwave Studio in order to investigate the wave propagation inside our NIM structure. Figure 7(a) shows the simulated NIM structure. We used the same parameters with the structure as shown in Fig. 1(a), but in this case with an alternative unit cell. The structure is excited with a plane wave with a wave-vector along the $+z$ direction using CST Microwave Studio. The E field is along the y axis and the H field is

along the x axis in the simulations. The structure had three unit cells along x and 5 unit cells along z .

We calculated the electric field profile by placing electric field monitors along the y axis at two different frequencies, 14.42 GHz and 17.00 GHz. 14.42 GHz was the frequency of the highest transmission within the negative-index regime for a five-layer NIM. Figure 7(b) shows the E field profile along the y direction, where the profile was calculated at the point $y=5$ mm. The wave propagates along the $+z$ direction in air. However, inside the fishnet structure, we observed backward wave propagation in the simulations (see video 1). The EM wave is guided through channels as shown with a dashed rectangular box in Fig. 7(a). We did not observe transmission through the wire pairs as clearly seen in the video. The wave propagation inside the metamaterial at 17.00 GHz is along the $+z$ direction (see video 2), since this frequency corresponds to the right-handed transmission regime where ϵ and μ are both positive.

5. Conclusion

We demonstrated backward wave propagation in a negative-index metamaterial at microwave frequencies. The advantages of our design are: (i) low-loss substrate in turn providing high transmission even for a five-layer NIM, (ii) negative-index behavior is present independent of the incident electromagnetic wave polarization, due to the symmetric configuration of the slab and wire pairs. We reported the highest transmission for a planar multi-layer metamaterial with a maximum value of transmission -3.7 dB for two-layers and -5.0 dB for five-layers. The retrieved parameters for single and two layer NIM structures differ. The absolute values of ϵ , μ , and n are higher for a one-layer NIM structure. A periodic structure, therefore, cannot be characterized by a single layer of a metamaterial unit. Additional parameters such as the lattice constant and geometric size need to be taken into account in order to make fair comparisons. Negative phase advance was experimentally verified by measuring the phase difference between those NIM structures with a different number of layers along the propagation direction. The transmitted phase decreases with an increase in the NIM size at the negative-index transmission band. Numerical simulations verified the backward wave propagation within the fishnet metamaterial at 14.42 GHz.

Acknowledgments

This work is supported by the European Union under the projects EU-METAMORPHOSE, EU-PHOREMOST, EU-PHOME, and EU-ECONAM, as well as TUBITAK under Project Numbers 105E066, 105A005, 106E198, and 106A017. One of the authors (E.O.) also acknowledges partial support from the Turkish Academy of Sciences.